

# Accepted Manuscript

Pharesinosides A-G, acylated glycosidic acid methyl esters derivatized by NH<sub>2</sub> silica gel on-column catalyzation from the crude resin glycosides of Pharbitis Semen

Li-Juan Bai, Jian-Guang Luo, Chen Chen, Ling-Yi Kong



PII: S0040-4020(17)30308-3

DOI: [10.1016/j.tet.2017.03.059](https://doi.org/10.1016/j.tet.2017.03.059)

Reference: TET 28565

To appear in: *Tetrahedron*

Received Date: 19 January 2017

Revised Date: 18 March 2017

Accepted Date: 21 March 2017

Please cite this article as: Bai L-J, Luo J-G, Chen C, Kong L-Y, Pharesinosides A-G, acylated glycosidic acid methyl esters derivatized by NH<sub>2</sub> silica gel on-column catalyzation from the crude resin glycosides of Pharbitis Semen, *Tetrahedron* (2017), doi: 10.1016/j.tet.2017.03.059.

This is a PDF file of an unedited manuscript that has been accepted for publication. As a service to our customers we are providing this early version of the manuscript. The manuscript will undergo copyediting, typesetting, and review of the resulting proof before it is published in its final form. Please note that during the production process errors may be discovered which could affect the content, and all legal disclaimers that apply to the journal pertain.

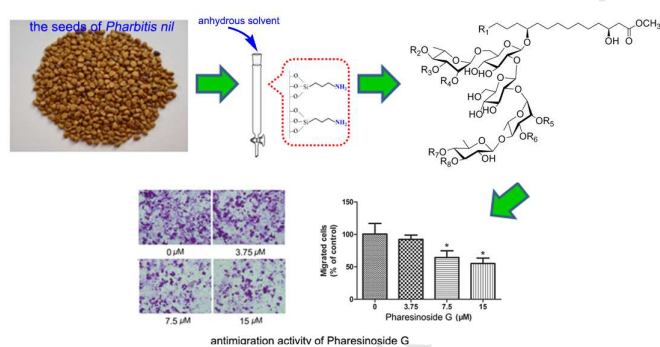
## Graphical Abstract

**Pharesinosides A-G, acylated glycosidic acid methyl esters derivatized by NH<sub>2</sub> silica gel on-column catalyzed from the crude resin glycosides of *Pharbitis Semen***

Leave this area blank for abstract info.

Li-Juan Bai, Jian-Guang Luo\*, Chen Chen and Ling-Yi Kong\*

*State Key Laboratory of Natural Medicines, Department of Natural Medicinal Chemistry, China Pharmaceutical University, 24 Tong Jia Xiang, Nanjing 210009, People's Republic of China*





Tetrahedron  
journal homepage: www.elsevier.com



## Pharesinosides A-G, acylated glycosidic acid methyl esters derivatized by NH<sub>2</sub> silica gel on-column catalyzation from the crude resin glycosides of *Pharbitis Semen*

Li-Juan Bai, Jian-Guang Luo\*, Chen Chen and Ling-Yi Kong\*

State Key Laboratory of Natural Medicines, Department of Natural Medicinal Chemistry, China Pharmaceutical University, 24 Tong Jia Xiang, Nanjing 210009, People's Republic of China

### ARTICLE INFO

#### Article history:

Received  
Received in revised form  
Accepted  
Available online

#### Keywords:

*Pharbitis nil*  
Convolvulaceae  
Resin glycosides  
Anti-tumor migration activity

### ABSTRACT

Application of NH<sub>2</sub> silica gel column chromatography using CH<sub>2</sub>Cl<sub>2</sub>-MeOH was found to show a satisfactory resolution for separation of the crude resin glycosides of *Pharbitis Semen* (the seeds of *Pharbitis nil*), led to the isolation of seven new acylated glycosidic acid methyl esters, Pharesinosides A-G (**1-7**), along with four known ones (**8-11**). These compounds (**1-11**) were considered to be generated via methyl esterification of the carboxyl group in acylated glycosidic acids. Their structures including stereochemistry were elucidated on the basis of a combination of the spectroscopic and chemical methods. All isolates were evaluated for anti-tumor migration activities with human colon cancer cell line HCT-116, and compound **7** exhibited a potent migration inhibitory activity.

2009 Elsevier Ltd. All rights reserved.

\* Corresponding author. Tel/fax: +86-25-8327-1405; luojg@cpu.edu.cn (Jian-Guang Luo)

\* Corresponding author. Tel/fax: +86-25-8327-1405; cpu\_lykong@126.com (Ling-Yi Kong)

## 1. Introduction

Resin glycosides, primarily isolated from the morning glory family (Convolvulaceae), are a class of unusual amphipathic secondary metabolites composed of hydrophobic (fatty acid aglycone) and hydrophilic (oligosaccharide) moieties.<sup>1</sup> The chemical structures are so complex and diverse that they exhibited various pharmacological activities, such as cytotoxic,<sup>2,3</sup> multidrug resistance (MDR) reversal<sup>4-6</sup> and antiviral<sup>7,8</sup> activities. Pharbitis Semen, the seeds of *Pharbitis nil*, is used as a purgative drug in Korea, China, and Japan.<sup>9</sup> Resin glycosides were reported to be responsible for its purgative property as traditional Chinese medicine.<sup>9</sup> Previous investigations on its crude resin glycosides have been confined to characterization of the glycosides acids and organic acids as alkaline hydrolysis products of the mixture for separation difficulties.<sup>10-12</sup> Recently, intact structures were disclosed by derivatization using indium (III) chloride in methanol. Seven oligoglycosides of hydroxyl fatty acid methyl esters were reported, involving 2-methyl-3-hydroxybutyric acid (nilic acid, Nla) and 2-methylbutyric acid (Mba) as esterifying moieties of the oligosaccharide core.<sup>13</sup> The existence of a free  $\beta$ -hydroxyl carboxylic acid moiety maybe resulted in the poor resolution of this type of acylated glycoside acids.<sup>13-15</sup> As part of our continuing endeavor to study on the novel active resin glycosides from plants in the Convolvulaceae,<sup>16-19</sup> we directed toward  $\text{CH}_2\text{Cl}_2$  emulsion layer of methanol extract of the seeds of *P. nil*. A satisfactory resolution of resin glycosides was achieved on  $\text{NH}_2$  silica gel using  $\text{CH}_2\text{Cl}_2$ -MeOH, finally resulting in the isolation of seven new acylated glycosidic acid methyl esters, Pharesinosides A-G (1-7), along with four known ones (8-11). Herein, we described their isolation and structure elucidation, as well as anti-tumor migration activity.

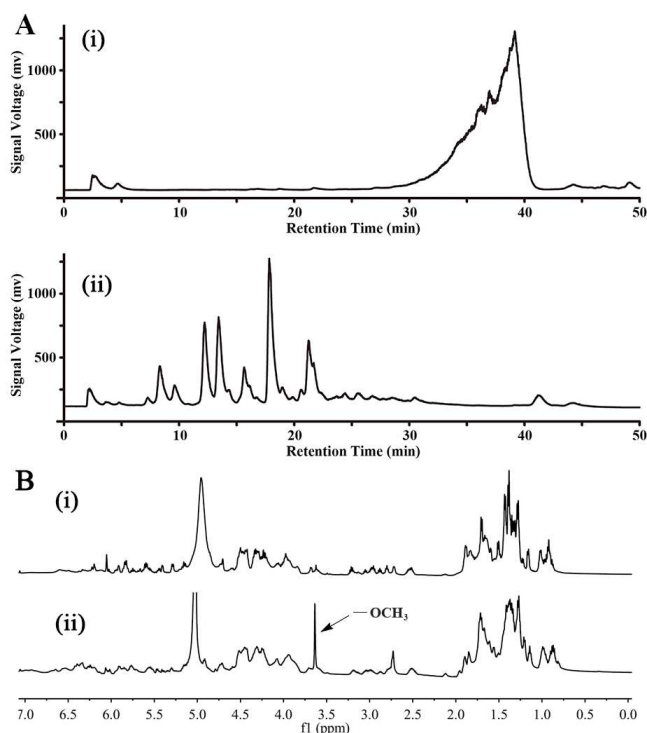


**Fig. 1.** HPLC (RP- $\text{C}_{18}$ )-ELSD (A) and  $^1\text{H}$  NMR (pyridine- $d_5$ ) (B) analysis of MeOH-soluble fraction (Fr. C) (i) and subfraction Cb (ii) from the seeds of *P. nil*.

## 2. Results and discussion

Attempted separation of MeOH-soluble fraction of  $\text{CH}_2\text{Cl}_2$  emulsion layer from the methanolic extract of the seeds of *P. nil*

by several methods (column chromatographies on silica gel, reversed-phase  $\text{C}_{18}$  (RP- $\text{C}_{18}$ ), MCI gel CHP 20P, Sephadex LH-20 and HPLC (Fig. 1A-i)) was not achieved. Inspired by the successful example,<sup>20</sup> the next fractionation of MeOH-soluble fraction (Fr. C) via a  $\text{NH}_2$  silica gel column chromatography (CC) with  $\text{CH}_2\text{Cl}_2$ -MeOH resulted in three subfractions (Ca, Cb and Cc). Subfraction Cb was rich in resin glycosides detected by  $^1\text{H}$  NMR spectrum, in which a remarkable methoxyl signal was arisen to suggest the methyl esterification of glycosidic acids (Fig. 1B-ii). Simultaneously, this subfraction was found to show a satisfactory resolution in the HPLC chromatogram (ELSD detector) (Fig. 1A-ii). Therefore, the subfraction Cb was further subjected to RP- $\text{C}_{18}$  and ultimately purified by preparative HPLC to yield pure compounds 1-11 (Fig. 2).

## 2.1. Structure elucidation

Compound 1 was obtained as colorless gum. Its molecular formula was deduced as  $\text{C}_{55}\text{H}_{96}\text{O}_{30}$  by HRESIMS data at  $m/z$  1259.5869 [ $\text{M} + \text{Na}$ ]<sup>+</sup> (calcd for  $\text{C}_{55}\text{H}_{96}\text{NaO}_{30}$ , 1259.5879). The  $^1\text{H}$  NMR spectrum showed signals assigned to two nilyl units, one methoxyl group, two nonequivalent methylene protons adjacent to a carbonyl group and three methyl groups assignable to 6-deoxyhexosyl units (Table 1). Five anomeric signals [ $\delta_{\text{H}}$  4.88 (1H, d,  $J = 7.6$  Hz), 5.86 (1H, d,  $J = 6.9$  Hz), 5.28 (1H, d,  $J = 6.8$  Hz), 5.35 (1H, s), 6.33 (1H, s);  $\delta_{\text{C}}$  103.1, 102.5, 106.1, 102.8, 102.2] in the NMR spectra (Tables 1 and 4) indicated that compound 1 was a pentasaccharide. The  $^1\text{H}$  and  $^{13}\text{C}$  NMR signals of the sugar moiety in 1 were assigned by comprehensive analysis of HSQC, HMBC and TOCSY spectra. Alkaline hydrolysis of 1 furnished nilic acid (15) and a glycosidic acid. The glycosidic acid was characterized as pharbitic acid C (12, Fig. 3) by comparison of  $^1\text{H}$  NMR and MS spectra with those of an authentic sample,<sup>12</sup> which was obtained from the alkaline hydrolysis products of the resin glycoside mixture (Fr. Cb). The connectivities of pharbitic acid C were further confirmed from the HMBC correlations: H-1 of Glc ( $\delta_{\text{H}}$  4.88) to C-11 ( $\delta_{\text{C}}$  81.5), H-1 of Qui ( $\delta_{\text{H}}$  5.28) to C-4 of Rha' ( $\delta_{\text{C}}$  84.5), H-1 of Rha' ( $\delta_{\text{H}}$  6.33) to C-2 of Glc' ( $\delta_{\text{C}}$  79.0), H-1 of Glc' ( $\delta_{\text{H}}$  5.86) to C-2 of Glc ( $\delta_{\text{C}}$  80.3), H-1 of Rha ( $\delta_{\text{H}}$  5.35) to C-6 of Glc ( $\delta_{\text{C}}$  68.8). The nilic acid was converted into *p*-bromophenacyl ester (17, Fig. 3), which was purified by HPLC and the (-)- $\alpha$ -methoxy- $\alpha$ -trifluoromethylphenylacetic acid (MTPA) ester of 17 was further obtained. On the other hand, after basic hydrolysis of Fr. Cb, the corresponding products (19) using the Mosher's method were gained, which proved to be a pair of (-)-MTPA esters of *p*-bromophenacyl nilate (19a:19b, approximate 4:1). Compared normal-phase HPLC analysis of (-)-MTPA ester of 17 with 19 (19a and 19b), one peak in (-)-MTPA ester of 17 with the same retention time as 19a confirmed the absolute configuration of 17 and nilic acid in the structure 1 was 2*R*, 3*R* (S44, Supplementary Data). Specification of ester linkage sites was established by the key HMBC correlations between protons of sugars and acyl carbons of the fatty acids, i.e. H-3 of Rha ( $\delta_{\text{H}}$  5.79) with C-1 of fragment A ( $\delta_{\text{C}}$  174.2). Finally, the location of methoxyl group was determined by the cross peak between the signal of  $\delta_{\text{H}}$  3.66 ( $\text{OCH}_3$ ) with  $\delta_{\text{C}}$  173.4 (C-1) (Fig. 4). Thus, the structure of compound 1 was identified as (3*S*, 11*S*)-dihydroxytetradecanoic acid methyl ester 11-*O*- $\beta$ -D-quinovopyranosyl-(1 $\rightarrow$ 4)-*O*- $\alpha$ -L-rhamnopyranosyl-(1 $\rightarrow$ 2)-*O*- $\beta$ -D-glucopyranosyl-(1 $\rightarrow$ 2)-*O*-{[3-*O*-3*R*-*O*-(3*R*-hydroxy-2*R*-methylbutyryl)-hydroxy-2*R*-methylbutyryl]- $\alpha$ -L-rhamnopyranosyl-(1 $\rightarrow$ 6)}-*O*- $\beta$ -D-glucopyranoside, named Pharesinoside A.

Compound 2, colorless gum, the molecular formula was determined as  $\text{C}_{56}\text{H}_{98}\text{O}_{32}$  based on the HRESIMS ion peak at  $m/z$  1305.5922 [ $\text{M} + \text{Na}$ ]<sup>+</sup> (calcd for  $\text{C}_{56}\text{H}_{98}\text{NaO}_{32}$ , 1305.5933). One

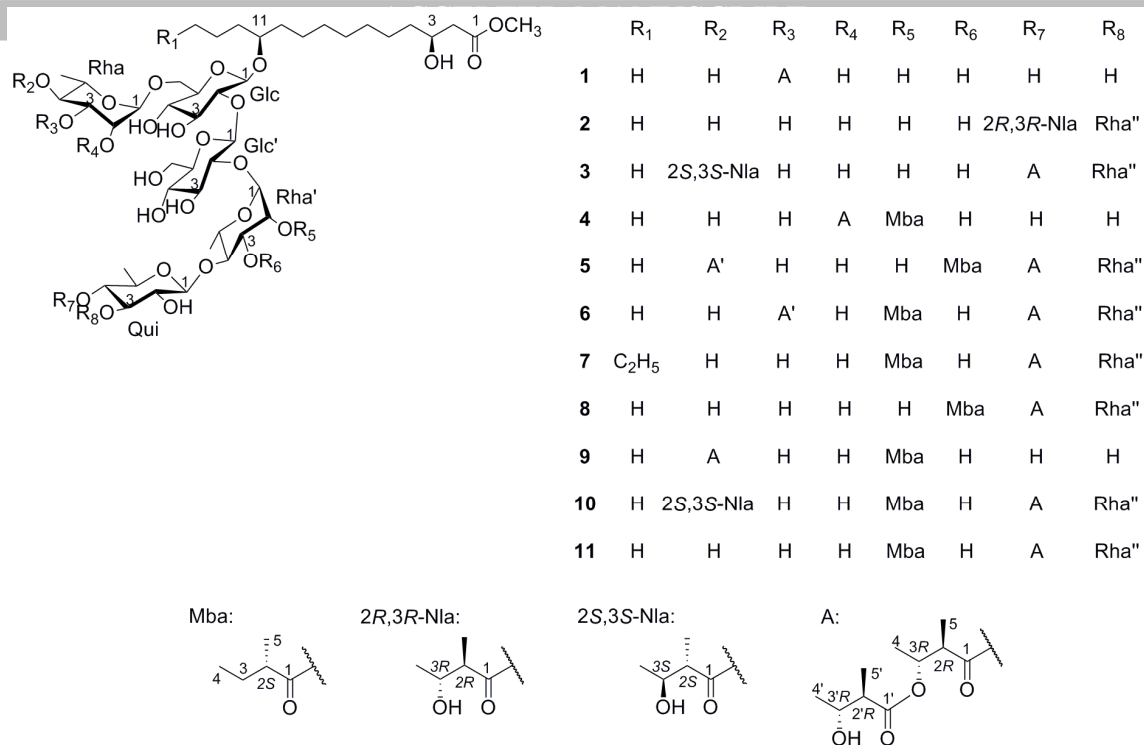


Fig. 2. Structures of compounds 1-11

nylyl unit, six anomeric protons  $\delta_{\text{H}}$  4.91 (d,  $J = 7.7\text{Hz}$ ), 5.88 (d,  $J = 6.3\text{Hz}$ ), 5.43 s, 6.31 s, 6.36 s, 5.16 (d,  $J = 7.8\text{Hz}$ ) and their corresponding carbon signals  $\delta_{\text{C}}$  103.1, 102.4, 102.8, 102.3, 101.6, 105.7 were observed in the  $^1\text{H}$  and  $^{13}\text{C}$  NMR spectra (Tables 1 and 4), indicating that **2** was a hexasaccharide and acylated by only one nilic acid. Basic hydrolysis of **2** afforded nilic acid and a glycosidic acid. The former was converted into the *p*-bromophenacyl ester and then purified by HPLC to give *p*-bromophenacyl nilate (**17'**). The comparison between the (-)-MTPA ester of **17'** and **19** in the normal-phase HPLC analysis indicated that (-)-MTPA ester of **17'** was same as **19a** and the absolute configuration of **17'** was 2*R*, 3*R*. Thus, nilic acid in the structure **2** was existed as 2*R*, 3*R*-form. The latter was identified as pharbitic acid (**13**) by comparison of the  $^1\text{H}$  NMR and MS spectra with those of an authentic sample.<sup>12</sup> The HMBC correlation from H-4 of Qui ( $\delta_{\text{H}}$  5.22) to C-1 of 2*R*, 3*R*-nilic acid ( $\delta_{\text{C}}$  175.4) suggested that nilic acid was connected to OH-4 of Qui. Therefore, the structure of compound **2** was determined as (3*S*, 11*S*)-dihydroxytetradecanoic acid methyl ester 11-*O*- $\alpha$ -L-rhamnopyranosyl-(1 $\rightarrow$ 3)-*O*-[4-*O*-(3*R*-hydroxyl-2*R*-methylbutyryl)]- $\beta$ -D-quinovopyranosyl-(1 $\rightarrow$ 4)-*O*- $\alpha$ -L-rhamnopyranosyl-(1 $\rightarrow$ 2)-*O*- $\beta$ -D-glucopyranosyl-(1 $\rightarrow$ 2)-*O*-[ $\alpha$ -L-rhamnopyranosyl-(1 $\rightarrow$ 6

)]-*O*- $\beta$ -D-glucopyranoside, named Pharesinoside B.

Compound **3**, a white, amorphous powder, gave a quasi-molecular ion at 1505.6970 [ $\text{M} + \text{Na}$ ]<sup>+</sup> (calcd for C<sub>66</sub>H<sub>114</sub>NaO<sub>36</sub>, 1505.6982) and the molecular formula was determined to be C<sub>66</sub>H<sub>114</sub>O<sub>36</sub>. The  $^1\text{H}$  NMR spectrum exhibited six methyl doublets between  $\delta_{\text{H}}$  1.28 and  $\delta_{\text{H}}$  1.43, three methine signals at  $\delta_{\text{H}}$  2.88-3.21, confirming the existence of three nilyl units in the structure (Table 1). The NMR spectra of **3** were similar to those of the known compound **10** except for the absence of a Mba unit. The alkaline hydrolysis product nilic acid was treated with *p*-bromophenacyl bromide and separated by pre-HPLC to give *p*-bromophenacyl nilate (**17''**). **17''** was further converted into (-)-MTPA ester and the analysis carried out in the normal-phase HPLC suggested that it was a (-)-MTPA ester mixture of (2*R*, 3*R*) and (2*S*, 3*S*) *p*-bromophenacyl nilate at the ratio of approximately 2:1, indicating that **17''** was a 2:1 mixture of *p*-bromophenacyl-(2*R*, 3*R*) nilate and its enantiomer and the structure **3** contained two 2*R*, 3*R*-nilic acid units and a 2*S*, 3*S*-nilic acid unit. These results were consistent with those of **10**. The esterification positions of the oligosaccharide core were elucidated via HMBC long-range couplings of  $\delta_{\text{H}}$  5.83 (H-4, Rha) with  $\delta_{\text{C}}$  176.0 (C-1,

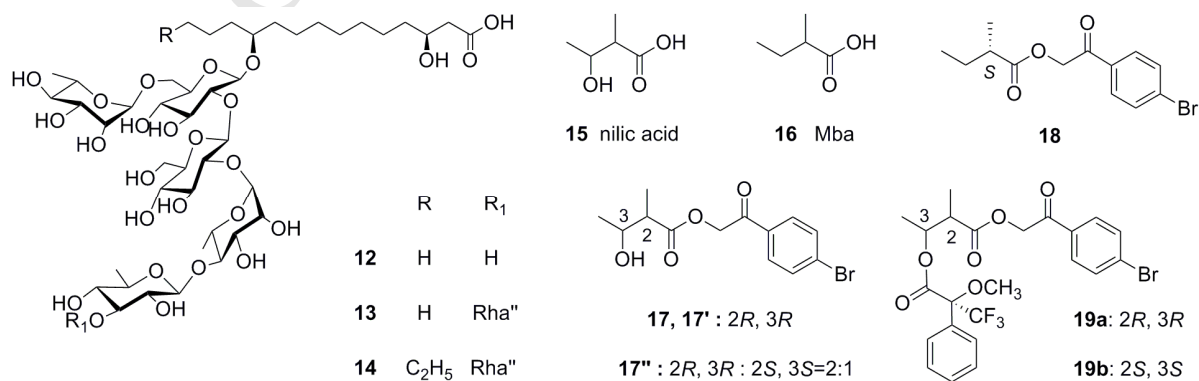


Fig. 3. Structures of compounds 12-19

**Table 1.**  $^1\text{H}$  NMR Data of Compounds **1-3** (500 MHz, in pyridine- $d_5$ )<sup>a</sup>

Position <sup>b</sup>	1	2	3	Position <sup>b</sup>	1	2	3
Glc-1	4.88 d (7.6)	4.91 d (7.7)	4.92 d (7.6)	Qui-1	5.28 d (6.8)	5.16 d (7.8)	5.14*
2	4.30 m*	4.33 m*	4.32 m*	2	4.02 m*	4.04 dd (8.5)	3.95 m*
3	4.52 dd (8.7)	4.50 m*	4.50 m*	3	4.11 m*	4.44 m*	4.25 m*
4	3.92 dd (8.8)	3.98 m*	3.95 m*	4	3.70 dd (8.3)	5.22 dd (9.5)	5.14 dd (9.5)
5	4.01 m*	4.01 m*	3.97 m*	5	3.66 m	3.55 dq (12.3, 6.1)	3.51 dq (12.5, 6.1)
6a	4.08 m*	4.10 m*	4.10 m*	6	1.57 d (6.0)	1.35 d (7.1)	1.28 d (7.1)
6b	4.47 m*	4.56 m*	4.49 m*	Ag-1			
Glc'-1	5.86 d (6.9)	5.88 d (6.3)	5.87 d (6.9)	2	2.73 m*	2.74 m*	2.74 m*
2	4.26 m*	4.23 m*	4.24 m*	3	4.45 m*	4.45 m*	4.50 m*
3	4.27 m*	4.23 m*	4.24 m*	11	3.95 m*	3.95 m*	3.95 m*
4	4.10 m*	4.10 dd (8.5)	4.10 m*	14	0.98 t (7.0)	0.99 t (7.0)	1.00 t (7.1)
5	3.88 m*	3.88 m*	3.86 m*	OCH <sub>3</sub>	3.66 s	3.64 s	3.64 s
6a	4.29 m*	4.30 m*	4.28 m*	A-1			
6b	4.45 m*	4.45 m*	4.22 m*	2	3.01 dq (7.0)		3.21 dq (7.2)
Rha-1	5.35 s	5.43 s	5.42 s	3	5.62 dq (6.5)		5.59 dq (6.5)
2	4.72 br s	4.51 m*	4.46 m*	4	1.35 d (6.5)		1.42 d (6.0)
3	5.79 m	4.51 m*	4.55 dd (9.8, 3.2)	5	1.21 d (6.6)		1.38 d (7.5)
4	4.41 m*	4.26 m*	5.83 dd (9.7)	A-1'			
5	4.39 m*	4.35 m*	4.35 m*	2'	2.76*		2.96 dq (6.9)
6	1.63 d (5.0)	1.68 d (6.1)	1.50 d (6.3)	3'	4.31 m*		4.42 m*
Rha'-1	6.33 s	6.31 s	6.29 s	4'	1.35 d (6.5)		1.39 d (6.0)
2	4.72 br s	4.70 br s	4.70 br s	5'	1.20 d (7.0)		1.28 d (7.1)
3	4.86 dd (9.4, 2.6)	4.76 dd (9.3, 3.3)	4.76 dd (9.3, 3.5)	2 <i>R</i> ,3 <i>R</i> -Nla-1			
4	4.45 m*	4.39 m*	4.37 m*	2		2.86 dq (7.5)	
5	5.05 dq (12.5, 6.2)	5.00 (12.5, 6.1)	5.04 m*	3		4.37 m*	
6	1.92 d (6.1)	1.86 d (6.3)	1.84 d (6.3)	4		1.36 d (6.9)	
Rha''-1		6.36 s	6.13 s	5		1.28 d (7.1)	
2		4.61 m*	4.73 br s	2 <i>S</i> ,3 <i>S</i> -Nla-1			
3		4.60 m*	4.46 m*	2			2.88 dq (7.0)
4		4.19 m*	4.28 m*	3			4.33 m*
5		4.35 m*	4.35 m*	4			1.43 d (6.5)
6		1.75 d (6.3)	1.73 d (6.1)	5			1.33 d (7.1)

<sup>a</sup> Chemical shifts ( $\delta$ ) are in ppm relative to TMS. The spin coupling ( $J$ ) is given in parentheses (Hz). Chemical shifts marked with asterisk (\*) indicate overlapped signals.

<sup>b</sup> Abbreviations: Glc = glucose; Rha = rhamnose; Mba = 2*S*-methylbutanoyl; Nla = 3-hydroxy-2-methylbutyryl; Ag = aglycone.

2*S*, 3*S*-nilic acid),  $\delta_{\text{H}}$  5.14 (H-4, Qui) with  $\delta_{\text{C}}$  173.1 (C-1, fragment A). Thus, the structure of **3** was elucidated as (3*S*, 11*S*)-dihydroxytetradecanoic acid methyl ester 11-*O*- $\alpha$ -L-rhamnopyranosyl-(1 $\rightarrow$ 3)-*O*-[4-*O*-3*R*-*O*-(3*R*-hydroxy-2*R*-methylbutyryl)-hydroxy-2*R*-methylbutyryl]- $\beta$ -D-quinovopyranosyl-(1 $\rightarrow$ 4)-*O*- $\alpha$ -L-rhamnopyranosyl-(1 $\rightarrow$ 2)-*O*- $\beta$ -D-glucopyranosyl-(1 $\rightarrow$ 2)-*O*-[4-*O*-(3*S*-hydroxy-2*S*-methylbutyryl)- $\alpha$ -L-rhamnopyranosyl-(1 $\rightarrow$ 6)]-*O*- $\beta$ -D-glucopyranoside, as Pharesinoside C.

Compound **4** was isolated as colorless gum and gave the molecular formula C<sub>60</sub>H<sub>104</sub>O<sub>31</sub>, as determined by HRESIMS  $m/z$  1343.6440 [M + Na]<sup>+</sup> (calcd for C<sub>60</sub>H<sub>104</sub>NaO<sub>31</sub>, 1343.6454). On the basis of alkaline hydrolysis, **4** yielded 2-methylbutyric acid (Mba, **16**), nilic acid and pharbitic acid C (**12**),<sup>12</sup> which were similar to compound **1** apart from the appearance of 2-methylbutyric acid. The difference also laid in the ester linkage sites

between protons of sugars and acyl carbons of the fatty acids. The key HMBC correlations: H-2 of Rha ( $\delta_{\text{H}}$  5.76) to C-1 of fragment A ( $\delta_{\text{C}}$  174.0), H-2 of Rha' ( $\delta_{\text{H}}$  5.93) to C-1 of Mba ( $\delta_{\text{C}}$  176.6), respectively, indicated the ester sites were at OH-2 Rha and OH-2 of Rha'. The absolute configuration of nilic acid was determined as 2*R*, 3*R* according to the aforementioned method. 2-methylbutyric acid was confirmed as *S* by comparison of optical rotation value of its *p*-bromophenacyl ester with *p*-bromophenacyl 2*S*-methylbutyrate (**18**), obtained from the resin glycoside mixture (Fr. Cb) and determined by  $^1\text{H}$  NMR spectrum and optical rotation value comparison with the literature.<sup>21</sup> Consequently, the structure of compound **4** was established as (3*S*, 11*S*)-dihydroxytetradecanoic acid methyl ester 11-*O*- $\beta$ -D-quinovopyranosyl-(1 $\rightarrow$ 4)-*O*-[2-*O*-(2*S*-methylbutyryl)]- $\alpha$ -L-rhamnopyranosyl-(1 $\rightarrow$ 2)- $\beta$ -D-glucopyranosyl-(1 $\rightarrow$ 2)-*O*-[2-*O*-3*R*-*O*-(3*R*-hydroxy-2*R*-methylbutyryl)-hydroxy-2*R*-methylbutyryl]- $\alpha$ -

**Table 2.** <sup>1</sup>H NMR Data of Compounds **4-6** (500MHz, in pyridine-*d*<sub>5</sub>)<sup>a</sup>

Position <sup>b</sup>	<b>4</b>	<b>5</b>	<b>6</b>	Position <sup>b</sup>	<b>4</b>	<b>5</b>	<b>6</b>
Glc-1	4.90 d (7.6)	4.88 d (7.7)	4.90 d (7.0)	4	3.70 m*	5.16 dd (9.5)	5.18 dd (9.5)
2	4.29 m*	4.18 m*	4.27 m*	5	3.71 m*	3.61 m	3.63 m
3	4.53 dd (8.7)	4.58 m*	4.48 m*	6	1.61 d (5.5)	1.30 d (7.0)	1.35 d (6.5)
4	3.94 m*	3.94 m*	3.94 m*	Ag-1			
5	3.94 m*	3.93 m*	3.99 m*	2	2.74 m	2.74 m	2.74*
6a	4.04 m*	4.14 m*	4.11 m*	3	4.43 m*	4.43 m*	3.36 m*
6b	4.44 m*	4.42 m*	4.45 m*	11	3.91 m*	3.96 m*	3.95 m*
Glc'-1	5.91 d (6.7)	5.71 d (7.1)	5.82 d (6.9)	14	1.03 t (7.1)	1.03 t (7.0)	1.01 t (7.1)
2	4.22 m*	4.25 m*	4.21 m*	OCH <sub>3</sub>	3.65 s	3.64 s	3.65 s
3	4.22 m*	4.22 m*	4.21 m*	A-1			
4	4.07 m*	4.06 dd (8.8)	4.08 dd (8.5)	2	3.04 dq (6.9)	3.22 dq (7.3)	3.22 dq (7.0)
5	3.85 m*	3.85 m*	3.81 m*	3	5.57 dq (6.5)	5.56 dq (6.5)	5.59 dq (6.5)
6a	4.29 m*	4.28 m*	4.28 m*	4	1.37 d (6.3)	1.42 d (6.0)	1.43 d (6.5)
6b	4.40 m*	4.45 m*	4.41 m*	5	1.28 d (7.1)	1.38 d (6.5)	1.39 d (6.5)
Rha-1	5.24 s	5.45 s	5.39 s	A-1'			
2	5.76 br s	4.36 m*	4.62 br s	2'	2.81 dq (7.0)	2.94 dq (6.8)	2.95 dq (7.0)
3	4.64 dd (9.5, 3.6)	4.50 m*	5.76 dd (9.1, 3.1)	3'	4.34 m*	4.45 m*	4.42 m*
4	4.14 dd (9.4)	5.76 dd (9.8)	4.39 m*	4'	1.35 d (6.3)	1.40 d (6.0)	1.38 d (6.0)
5	4.37 dd (9.5, 6.2)	4.36 m*	4.41 m*	5'	1.25 d (7.1)	1.30 d (7.0)	1.28 d (6.9)
6	1.69 d (6.3)	1.52 d (6.3)	1.68 d (5.8)	A'-1			
Rha'-1	6.24 s	6.33 s	6.20 s	2		3.02 dq (7.1)	3.02 dq (7.0)
2	5.93 br s	4.72 br s	5.93 br s	3		5.53 dq (6.5)	5.60 dq (6.0)
3	5.00 dd (9.4, 3.6)	6.23 dd (9.6, 2.9)	4.99 dd (9.5, 3.6)	4		1.36 d (6.3)	1.34 d (6.5)
4	4.32 m*	4.56 dd (9.5)	4.28 m*	5		1.30 (7.0)	1.24 d (7.0)
5	5.12 m	5.18 dd (9.5)	5.07 m	A'-1'			
6	1.96 d (6.1)	1.84 d (6.0)	1.90 d (6.1)	2'		2.78 dq (7.1)	2.78*
Rha''-1		6.02 s	6.06 s	3'		4.39 m*	4.31 m*
2		4.74 br s	4.71 br s	4'		1.35 d (6.3)	1.33 d (6.5)
3		4.48 m*	4.45 m*	5'		1.27 d (6.9)	1.23 d (7.0)
4		4.21 m*	4.23 m*	Mba-1			
5		4.34 m*	4.29 m*	2	2.51 ddq (7.0)	2.54 ddq (7.1)	2.52 ddq (7.0)
6		1.71 d (6.1)	1.70 d (6.1)	3a	1.50 m*	1.45 *	1.53 m*
Qui-1	5.34 <sup>c</sup>	4.94 m*	5.30 d (7.9)	3b	1.78 m*	1.87 *	1.81 m*
2	4.05 m*	3.88 m*	3.99 m*	4	0.91 dd (7.3)	0.88 dd (7.4)	0.93 dd (7.4)
3	4.07 m*	4.18 m*	4.23 m*	5	1.15 d (6.9)	1.22 d (7.7)	1.17 d (6.9)

<sup>a</sup> Chemical shifts ( $\delta$ ) are in ppm relative to TMS. The spin coupling ( $J$ ) is given in parentheses (Hz). Chemical shifts marked with asterisk (\*) indicate overlapped signals.

<sup>b</sup> Abbreviations: Glc = glucose; Rha = rhamnose; Mba = 2S-methylbutanoyl; Nla = 3-hydroxy-2-methylbutyryl; Ag = aglycone.

<sup>c</sup> Signal is deformed by virtual coupling

L-rhamnopyranosyl-(1 $\rightarrow$ 6)]-*O*- $\beta$ -D-glucopyranoside, named Pharesinoside D.

Compounds **5** and **6** shared the same molecular formula C<sub>76</sub>H<sub>130</sub>O<sub>39</sub> based on the [M + Na]<sup>+</sup> HRESIMS ions at  $m/z$  1689.8066 and 1689.8073, respectively. The same alkaline hydrolysis products, nilic acid, 2-methylbutyric acid and pharbitic acid D (**13**)<sup>12</sup> suggested that they were the positional isomers. Comparison of the NMR data (Tables 2 and 4) of compounds **5** and **6** showed the existence of four nilyl units, one Mba unit and the major difference was that two downshift non-

anomeric proton signals were placed at H-4 of Rha, H-3 of Rha' in **5**, while at H-3 of Rha and H-2 of Rha' in **6**. A further analysis of HMBC led to assignments of the exact locations of the acyl groups on the oligosaccharide skeletons: from H-4 of Rha ( $\delta_{\text{H}}$  5.76) to C-1 of fragment A' ( $\delta_{\text{C}}$  174.0), from H-3 of Rha' ( $\delta_{\text{H}}$  6.23) to C-1 of Mba ( $\delta_{\text{C}}$  177.2) and from H-4 of Qui ( $\delta_{\text{H}}$  5.16) to C-1 of fragment A ( $\delta_{\text{C}}$  173.2) in **5** suggested that the ester linkages were located at OH-4 of Rha, OH-3 of Rha' and OH-4 of Qui, while at OH-3 of Rha, OH-2 of Rha' and OH-4 of Qui in compound **6**. The absolute configurations of all nilic and 2-

**Table 3.**  $^1\text{H}$  NMR Data of Compound **7** (500MHz, in pyridine- $d_5$ )<sup>a</sup>

Position <sup>b</sup>	<b>7</b>	Position <sup>b</sup>	<b>7</b>
Glc-1	4.94 d (7.6)	5	4.35 m*
2	4.32 m*	6	1.70 d (6.1)
3	4.51 m*	Qui-1	5.30 d (7.9)
4	3.94 m*	2	4.00 m*
5	3.99 m*	3	4.24 m*
6a	4.12 m*	4	5.15 dd (9.5)
6b	4.55 m*	5	3.61 m
Glc'-1	5.87 d (7.1)	6	1.34 d (6.2)
2	4.23 m*	Ag-1	
3	4.22 m*	2	2.73 m
4	4.09 dd (8.5)	3	4.43 m*
5	3.84 m*	11	3.96 m*
6a	4.29 m*	16	0.89 t (7.5)
6b	4.44 m*	OCH <sub>3</sub>	3.65 s
Rha-1	5.46 s	A-1	
2	4.49 m*	2	3.20 dq (7.0)
3	4.49 m*	3	5.58 dq (6.5)
4	4.23 m*	4	1.41 d (6.3)
5	4.34 m*	5	1.37 d (6.2)
6	1.67 d (6.1)	A-1'	
Rha'-1	6.23 s	2'	2.97 dq (6.6)
2	5.91 br s	3'	4.45 m*
3	4.99 dd (9.2, 3.0)	4'	1.39 d (6.3)
4	4.30 m*	5'	1.28 d (7.0)
5	5.09 m	Mba-1	
6	1.90 d (6.1)	2	2.52 ddq (7.0)
Rha''-1	6.05 s	3a	1.53 m*
2	4.73 br s	3b	1.81 m*
3	4.48 m*	4	0.91 dd (7.5)
4	4.22 m*	5	1.16 d (7.0)

<sup>a</sup> Chemical shifts ( $\delta$ ) are in ppm relative to TMS. The spin coupling ( $J$ ) is given in parentheses (Hz). Chemical shifts marked with asterisk (\*) indicate overlapped signals.

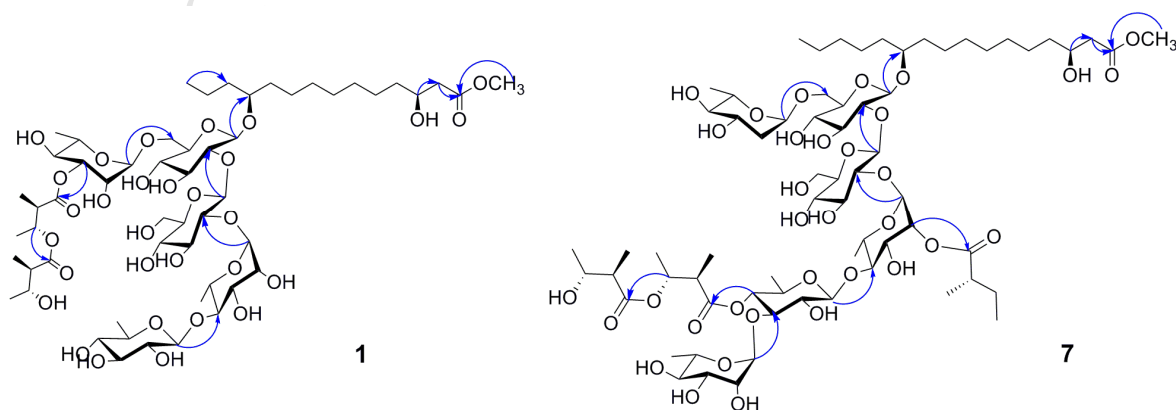
<sup>b</sup> Abbreviations: Glc = glucose; Rha = rhamnose; Mba = 2S-methylbutanoyl; Nla = 3-hydroxy-2-methylbutyryl; Ag = aglycone.

methylbutyric acids in **5** and **6** were determined to be 2*R*, 3*R* and 2*S*, respectively, using the foregoing mentioned method. Therefore, the structures of compounds **5** and **6** were established as depicted.

Compound **7**, obtained as white amorphous powders, gave the HRESIMS quasimolecular ion of  $[\text{M} + \text{Na}]^+$  at  $m/z$  1517.7340 and the molecular formula was assigned as  $\text{C}_{68}\text{H}_{118}\text{O}_{35}$ . The NMR spectra of **7** showed close similarity with the known compound PM-3,<sup>13</sup> except for the esterification position of Mba unit at the oligosaccharide core. The same basic hydrolysis products, nilic acid, 2-methylbutyric acid and pharbitic acid B (**14**)<sup>12</sup> suggested that they were positional isomers like **5** and **6**. A long-range correlation between H-2 of Rha' ( $\delta_{\text{H}}$  5.91) and C-1 of Mba unit ( $\delta_{\text{C}}$  176.6) indicated that the exact position of Mba unit was at OH-2 of Rha' (Fig. 4). Thus the structure of **7** was defined as (3*S*, 11*S*)-dihydroxyhexadecanoic acid methyl ester 11-*O*- $\alpha$ -L-rhamnopyranosyl-(1 $\rightarrow$ 3)-*O*-[4-*O*-3*R*-*O*-(3*R*-hydroxy-2*R*-methylbutyryl)-hydroxy-2*R*-methylbutyryl]- $\beta$ -D-quinovopyranosyl-(1 $\rightarrow$ 4)-*O*-[2-*O*-(2*S*-methylbutyryl)]- $\alpha$ -L-rhamnopyranosyl-(1 $\rightarrow$ 2)-*O*- $\beta$ -D-glucopyranosyl-(1 $\rightarrow$ 2)-*O*-[ $\alpha$ -L-rhamnopyranosyl-(1 $\rightarrow$ 6)]-*O*- $\beta$ -D-glucopyranoside.

Four known compounds **8-11** were also isolated from the crude resin glycosides of the seeds of *P. nil*. Their structures were identified by comparison of  $^1\text{H}$ ,  $^{13}\text{C}$  NMR and HRESIMS data with those of the literature.<sup>13</sup>

Although the isolation of a pure form could not be achieved, we further illustrated the detailed structures of the crude resin glycosides of Pharbitis Semen. These resin glycosides of Pharbitis Semen are naturally existed to be a mixture of monomers composed of free carboxylic acid forms, which resulted in poor resolution of these compounds.<sup>13</sup> Such acylated glycosidic acids possess a polar free  $\beta$ -hydroxyl carboxylic acid headgroup linked to a hydrophobic alkyl tail (alkyl chain and acylated glycosidic core). As amphiphilic molecules, they are capable of demonstrating liquid crystalline phase behavior and forming micelle systems.<sup>22</sup> Since the intermolecular hydrogen bonds between headgroups (free  $\beta$ -hydroxyl carboxylic acid) make the micelle be stable, the acylated glycosidic acids are difficult to be separated in the aqueous solution.<sup>23</sup> Therefore, for HPLC analysis (RP-C<sub>18</sub>, MeOH-H<sub>2</sub>O or CH<sub>3</sub>CN-H<sub>2</sub>O), the acylated glycosidic acid mixture exhibited an inseparable broad peak with larger retention time (Fig. 1A-i), while the acylated glycosidic acid methyl ester mixture (the polar free carboxylic acid headgroups were destroyed) showed a satisfactory resolution and smaller retention time (Fig. 1A-ii). Additionally, NH<sub>2</sub> silica gel may serve as a potential alkaline catalyst leading to methyl

**Fig. 4.** Key HMBC correlations of compounds **1** and **7****Table 4.**  $^{13}\text{C}$  NMR Data of Compounds **1-7** (125 MHz, in pyridine- $d_5$ )<sup>a</sup>

Position <sup>b</sup>	1	2	3	4	5	6	7	Position <sup>b</sup>	1	2	3	4	5	6	7
Glc-1	103.1	103.1	103.1	103.2	103.2	103.1	103.2	CH <sub>2</sub>	35.4	35.5	35.5	35.5	35.4	35.4	35.3
2	80.3	80.0	80.2	80.0	80.4	80.1	80.2	CH <sub>2</sub>	31.1	31.0	31.0	31.0	31.1	31.1	32.8
3	79.6	79.8	79.7	79.7	79.1	79.7	79.7	CH <sub>2</sub>	30.7	30.7	30.7	30.7	30.7	30.7	31.0
4	72.6	72.3	72.2	72.0	71.8	72.3	72.3	CH <sub>2</sub>	30.7	30.6	30.6	30.6	30.6	30.6	30.7
5	76.7	76.7	76.6	76.3	76.5	76.7	76.9	CH <sub>2</sub>	26.7	26.7	26.7	26.7	26.7	26.7	30.6
6	68.8	68.5	68.7	68.7	68.6	68.8	68.6	CH <sub>2</sub>	25.7	25.8	25.8	25.7	25.4	25.7	26.7
Glc'-1	102.5	102.4	102.4	102.1	102.9	102.3	102.2	CH <sub>2</sub>	19.6	19.5	19.5	19.5	19.1	19.5	25.9
2	79.0	79.4	79.6	78.5	78.0	79.1	78.8	CH <sub>2</sub>							25.8
3	79.7	79.7	79.6	80.0	79.8	79.3	79.4	CH <sub>2</sub>							23.4
4	73.0	73.0	73.0	73.0	73.1	73.0	73.0	A-1	174.2		173.1	174.0	173.2	173.1	173.2
5	78.2	78.2	78.1	78.3	77.9	78.1	78.2	2	45.3		44.8	45.3	44.8	44.7	44.8
6	63.7	63.6	63.6	63.6	63.9	63.6	63.6	3	71.9		71.3	71.9	71.4	71.4	71.4
Rha-1	102.8	102.8	102.8	99.3	102.8	102.9	102.9	4	16.9		17.3	17.3	17.2	17.2	17.3
2	70.1	72.8	72.4	74.5	72.8	70.0	72.7	5	12.9		13.2	13.2	13.4	13.1	13.2
3	76.8	73.2	71.0	70.8	70.9	76.8	73.1	A-1'	175.2		175.2	175.2	175.2	175.3	175.2
4	71.4	74.6	76.0	74.7	76.0	71.2	74.5	2'	49.1		48.6	49.0	48.5	48.6	48.6
5	70.4	70.2	67.5	70.1	67.5	70.3	70.1	3'	69.5		69.2	69.4	69.2	69.2	69.2
6	19.1	19.1	18.7	19.0	18.8	19.3	19.2	4'	21.3		20.7	21.2	20.5	20.6	20.5
Rha'-1	102.2	102.3	102.4	98.9	101.4	99.0	98.9	5'	13.8		12.8	13.5	12.6	12.8	12.7
2	72.5	72.5	72.8	73.7	71.4	73.8	73.8	2 <i>R</i> ,3 <i>R</i> -Nla-1		175.4					
3	72.9	72.8	72.9	70.5	75.2	70.4	70.5	2		49.6					
4	84.5	84.6	84.5	84.7	78.4	83.8	83.6	3		69.3					
5	68.4	68.4	68.3	68.1	68.4	68.1	68.0	4		21.5					
6	19.3	19.2	19.2	19.3	19.2	19.1	19.2	5		14.9					
Rha''-1		101.6	102.7		102.9	102.8	102.9	2 <i>S</i> ,3 <i>S</i> -Nla-1			176.0				
2		72.6	72.5		73.0	72.8	72.9	2			49.0				
3		72.5	72.8		72.8	72.8	72.7	3			70.2				
4		74.9	74.4		74.5	74.4	74.4	4			70.2				
5		69.9	70.5		70.4	70.4	70.4	5			13.8				
6		19.2	19.3		19.4	19.2	19.3	A'-1					174.0	174.0	
Qui-1	106.1	105.7	105.5	106.1	104.3	105.2	105.1	2					45.5	45.2	
2	76.7	77.7	77.1	76.7	76.1	76.7	77.0	3					71.7	71.8	
3	78.6	77.2	80.0	78.5	80.4	80.0	80.3	4					17.4	16.9	
4	77.2	74.7	75.2	77.1	75.4	75.3	75.3	5					18.8	12.7	
5	73.5	71.2	70.9	73.6	70.7	70.9	70.9	A'-1'					175.1	175.2	
6	19.0	18.6	18.7	19.2	18.6	18.7	18.7	2'					49.0	49.0	
Ag-1	173.4	173.4	173.4	173.4	173.4	173.4	173.4	3'					69.3	69.5	
2	43.9	43.9	43.9	43.9	43.9	43.9	43.9	4'					21.2	21.3	
3	68.8	68.8	68.7	69.4	68.7	68.1	68.7	5'					13.6	13.8	
11	81.5	81.5	81.3	81.6	81.2	81.5	81.8	Mba-1				176.6	177.2	176.6	176.6
14	15.1	15.1	15.1	15.1	15.1	15.1		2				41.8	42.2	41.8	41.8
16								3				27.5	27.1	27.5	27.5
OCH <sub>3</sub>	51.8	51.8	51.7	51.7	51.7	51.7	51.7	4				12.1	12.3	12.1	12.1
CH <sub>2</sub>	38.6	38.6	38.6	38.6	38.6	38.6	38.6	5				17.2	17.1	17.3	17.2
CH <sub>2</sub>	38.2	38.2	38.2	38.1	38.1	38.1	35.9								

<sup>a</sup> Chemical shifts ( $\delta$ ) are in ppm relative to TMS. The spin coupling ( $J$ ) is given in parentheses (Hz). Chemical shifts marked with asterisk (\*) indicate overlapped signals.

<sup>b</sup> Abbreviations: Glc = glucose; Rha = rhamnose; Mba = 2*S*-methylbutanoyl; Nla = 3-hydroxy-2-methylbutyryl; Ag = aglycone

esterification of carboxylic acid groups by using  $\text{CH}_2\text{Cl}_2$ -MeOH,<sup>24-27</sup> which facilitated the isolation and structure illustration of acylated glycosidic acids from *Pharbitis Semen*. Interestingly, solid-supported  $\text{NH}_2$  materials have been used for an environmentally friendly and reusable solid-base catalyst for some condensation reactions in anhydrous conditions due to its high surface area and its functionalized pore channels of large diameter.<sup>24,28-30</sup> The present  $\text{NH}_2$  silica gel-catalyzed methyl esterification of carboxylic acids is considered useful for the isolation of carboxylic acid containing compounds from complex mixtures.

The isolated compounds were evaluated for cytotoxic activities against MDA-MB-231 human breast cancer cell lines and HCT-116 human colon cancer cell lines. The results showed that compounds were inactive against two cell lines ( $\text{IC}_{50} > 100 \mu\text{M}$ ), except for **5**, **7** with weak cytotoxic activities towards HCT-116 cells ( $\text{IC}_{50} = 35.17 \pm 1.56$  and  $27.53 \pm 1.05 \mu\text{M}$ , respectively). Oxaliplatin was used as the positive control with  $\text{IC}_{50}$  values of  $8.65 \pm 1.62 \mu\text{M}$  and  $3.95 \pm 0.96 \mu\text{M}$  towards MDA-MB-231 and HCT-116 cell lines.

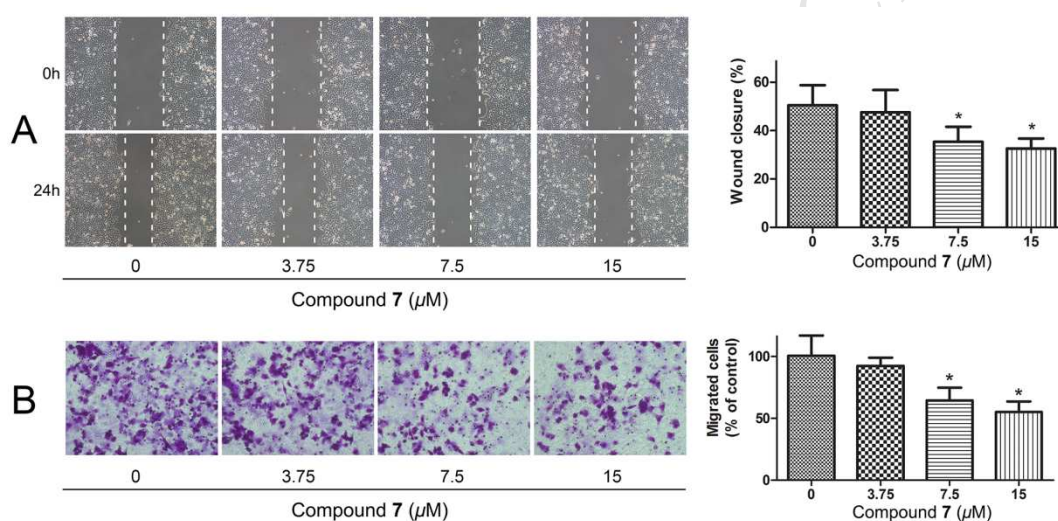


Fig. 6. Wound healing and transwell assay on HCT-116 cells with compound 7 in different concentrations.

The individual compounds were further screened for their inhibitory effects on migration of cancer cells through wound healing assay with HCT-116 cells. Among the tested compounds, compound **7** exhibited preferential activity (Fig. 5), demonstrating that the  $\text{C}_{16}$  aglycone in **7** is important for the observed activity. Detailed assays by transwell and wound healing indicated that compound **7** suppressed cell migration effectively in a dose dependent manner (Fig. 6). These data suggest that **7** represents a potential tumor migration inhibitory agent.

## 2.2. Conclusion

In summary, 11 compounds including 7 new and 4 known resin glycoside methyl esters, which were considered to be generated via methyl esterification by  $\text{NH}_2$  silica gel CC with  $\text{CH}_2\text{Cl}_2$ -MeOH, were isolated and identified from the seeds of *P. nil*. Although the separation of pure compounds from the crude resin glycosides of *P. nil* was not succeeded, it provided a convenient and useful sample processing method to solve the separation problems. Moreover, the anti-tumor migration bioactivity of these compounds was reported for the first time, which makes for the enrichment of pharmacological activity of resin glycosides. Notably, the structure characteristics in the compounds make further investigations on the mechanisms of action of these compounds be of value for biological, chemical

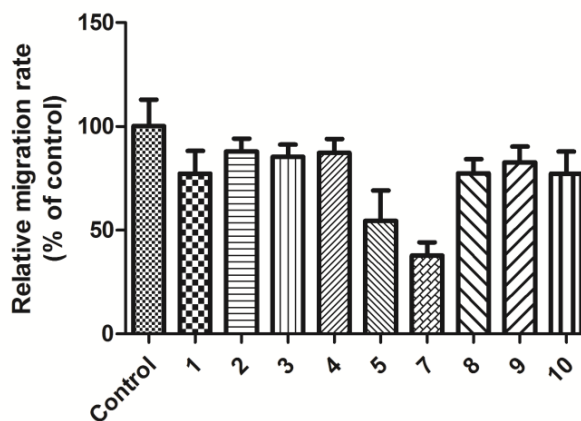


Fig. 5. Effect of individual compounds on HCT-116 cells migration.

and analytical applications (for chiral recognition), or as biomaterials.<sup>31</sup>

## Experimental Section

### 3.1. General experimental procedures

Optical rotations were measured with a JASCO P-1020 polarimeter. IR spectra were recorded in KBr-disc on a Bruker Tensor 27 spectrometer. 1D and 2D NMR spectra were recorded on a Bruker AVIII-500 NMR instrument in pyridine- $d_5$  at 500 MHz ( $^1\text{H}$ ) and 125 MHz ( $^{13}\text{C}$ ), and chemical shifts were recorded as  $\delta$  values. Mass experiments were performed on an Agilent 1100 Series LC/MSD ion-trap mass spectrometer (ESIMS) and Agilent 6520B Q-TOF spectrometer (HRESIMS), respectively. Column chromatography (CC) was carried out using silica gel (Qingdao Haiyang Chemical Co., Ltd.), MCI gel CHP 20P (Mitsubishi Chemical Corp., Tokyo, Japan), Sephadex LH-20 (75-150  $\mu\text{m}$ , Pharmacia, Sweden),  $\text{NH}_2$  silica gel (40-75  $\mu\text{m}$ , Fuji Silysia Chemical Ltd, Japan) and RP-C<sub>18</sub> (40-63  $\mu\text{m}$ , Fuji, Japan). Thin-layer chromatography was performed on pre-coated silica gel GF254 plates (Qingdao Marine Chemical Co., Ltd., China) and detected by spraying with 10%  $\text{H}_2\text{SO}_4$ -EtOH. Analytical reversed-phase and normal-phase HPLC were determined on an Agilent 1100 series system with an Agilent Eclipse XDB-C<sub>18</sub> column (150  $\times$  4.6 mm, 5  $\mu\text{m}$ ) and Shimadzu

LC-2010CHT series system with a Welch Ultimate SiO<sub>2</sub> column M1317 [M + Cl]<sup>-</sup> and 1300 [M + NH<sub>4</sub>]<sup>+</sup>; HRESIMS *m/z* 1305.5922 [M + Na]<sup>+</sup> (calcd for C<sub>56</sub>H<sub>98</sub>NaO<sub>32</sub>, 1305.5933).

### 3.2. Plant material

The dried seeds of *P. nil* were purchased from Hebei province of China in April 2014, and were authenticated by Professor Min-Jian Qin, Department of Medicinal Plants, China Pharmaceutical University. A voucher specimen (No. 2014-PBC) is deposited in the Department of Natural Medicinal Chemistry, China Pharmaceutical University.

### 3.3. Extraction and isolation

The dried and powdered seeds of *P. nil* (500 g) were extracted with ultrasonication in MeOH (2 l × 4). After removal of solvent, the residue (47.1 g) was suspended in H<sub>2</sub>O and successively extracted with petroleum ether (Fr. A), CH<sub>2</sub>Cl<sub>2</sub> (Fr. B), EtOAc (Fr. D) and *n*-BuOH (Fr. E). Serious emulsification appeared when extracted with CH<sub>2</sub>Cl<sub>2</sub> and no effective methods to break it. Emulsion layer was dissolved in MeOH (45 ml) with sonication for 10 min, then stand overnight to afford MeOH-soluble (Fr. C) and -insoluble (Fr. C') fractions. Fr. C (14 g) was chromatographed over a NH<sub>2</sub> silica gel CC and eluted with a step gradient CH<sub>2</sub>Cl<sub>2</sub>-MeOH (5:1-0:1, *v/v*) to get fractions Ca, Cb and Cc, monitored by HPLC (ELSD) and TLC. The elution condition of HPLC-ELSD analysis of MeOH-soluble fraction (Fr. C) and subfraction Cb was: 0 min, 70% MeOH; 15 min, 80% MeOH; 25 min, 85% MeOH; 35 min, 90% MeOH; 40 min, 100% MeOH; 50min, 100% MeOH. Fr. Cb was rich in resin glycosides and run on an open RP-C<sub>18</sub> CC with a continuous gradient of MeOH-H<sub>2</sub>O (6:4 to 10:0) to afford eight fractions (Fr. Cb1-8). Fr. Cb2 was further subjected to a RP-C<sub>18</sub> CC with a gradient elution (MeOH-H<sub>2</sub>O, 5:5 to 10:0, *v/v*) followed by preparative HPLC using CH<sub>3</sub>CN-H<sub>2</sub>O (33:67, *v/v*) with 0.1% formic acid to give **1** (19.9 mg) and **2** (10.3 mg). Fr. Cb4 was submitted to a RP-C<sub>18</sub> CC using a step gradient of CH<sub>3</sub>CN-H<sub>2</sub>O to give seven subfractions (Fr. Cb4a-g). Fr. Cb4b and Fr. Cb4e were purified by preparative HPLC with MeOH-H<sub>2</sub>O (74:26, *v/v*) to yield compounds **3** (15.5 mg), **8** (8.7 mg) and **9** (14.2 mg). Separation of Fr. Cb4d was achieved by preparative HPLC with CH<sub>3</sub>CN-H<sub>2</sub>O (41:59, *v/v*) adding 0.1% formic acid to afford compound **4** (12.1 mg). Fr. Cb6 was directly separated by preparative HPLC using MeOH-H<sub>2</sub>O (80:20, *v/v*) as mobile phase to furnish compound **11** (41.7mg). Fr. Cb7 was further performed on a RP-C<sub>18</sub> CC and **5** (11.1 mg) was obtained from subfraction Cb7b through the preparative HPLC (MeOH-H<sub>2</sub>O, 80:20, *v/v*); Compounds **6** (14.5 mg), **7** (11.7 mg) and **10** (10.3 mg) were obtained successively from subfractions Cb7f, Cb7h, Cb7g through the preparative HPLC with 50% CH<sub>3</sub>CN in water.

### 3.4. Characteristics of compounds

**3.4.1. Pharesinoside A (1).** Colorless gum; [α]<sub>D</sub><sup>25</sup> -21.8 (*c* 1.0, MeOH); IR (KBr) *v*<sub>max</sub> 3439, 2931, 1727, 1633, 1454, 1384, 1073 cm<sup>-1</sup>; <sup>1</sup>H and <sup>13</sup>C NMR data, see Tables 1 and 4; ESIMS *m/z* 1271 [M + Cl]<sup>-</sup> and 1254 [M + NH<sub>4</sub>]<sup>+</sup>; HRESIMS *m/z* 1259.5869 [M + Na]<sup>+</sup> (calcd for C<sub>55</sub>H<sub>96</sub>NaO<sub>30</sub>, 1259. 5879).

**3.4.2. Pharesinoside B (2).** Colorless gum; [α]<sub>D</sub><sup>25</sup> -59.6 (*c* 1.3, MeOH); IR (KBr) *v*<sub>max</sub> 3419, 2932, 1729, 1631, 1452, 1384, 1070 cm<sup>-1</sup>; <sup>1</sup>H and <sup>13</sup>C NMR data, see Tables 1 and 4; ESIMS *m/z*

**3.4.3. Pharesinoside C (3).** White amorphous powder; [α]<sub>D</sub><sup>25</sup> -51.3 (*c* 1.3, MeOH); IR (KBr) *v*<sub>max</sub> 3428, 2929, 2854, 1732, 1643, 1455, 1384, 1073 cm<sup>-1</sup>; <sup>1</sup>H and <sup>13</sup>C NMR data, see Tables 1 and 4; ESIMS *m/z* 1505 [M + Na]<sup>+</sup> and 1517 [M + Cl]<sup>-</sup>; HRESIMS *m/z* 1505.6970 [M + Na]<sup>+</sup> (calcd for C<sub>66</sub>H<sub>114</sub>NaO<sub>36</sub>, 1505. 6982).

**3.4.4. Pharesinoside D (4).** Colorless gum; [α]<sub>D</sub><sup>25</sup> -17.1 (*c* 1.1, MeOH); IR (KBr) *v*<sub>max</sub> 3436, 2931, 1729, 1632, 1454, 1383, 1073 cm<sup>-1</sup>; <sup>1</sup>H and <sup>13</sup>C NMR data, see Tables 2 and 4; ESIMS *m/z* 1343[M + Na]<sup>+</sup> and 1355[M + Cl]<sup>-</sup>; HRESIMS *m/z* 1343.6440 [M + Na]<sup>+</sup> (calcd for C<sub>60</sub>H<sub>104</sub>NaO<sub>31</sub>, 1343.6454).

**3.4.5. Pharesinoside E (5).** Colorless gum; [α]<sub>D</sub><sup>25</sup> -28.8 (*c* 1.5, MeOH); IR (KBr) *v*<sub>max</sub> 3448, 2927, 1728, 1639, 1384, 1075 cm<sup>-1</sup>; <sup>1</sup>H and <sup>13</sup>C NMR data, see Tables 2 and 4; ESIMS *m/z* 1701 [M + Cl]<sup>-</sup> and 1689 [M + NH<sub>4</sub>]<sup>+</sup>; HRESIMS *m/z* 1689.8066 [M + Na]<sup>+</sup> HRESIMS *m/z* 1689.8066 [M + Na]<sup>+</sup> (calcd for C<sub>76</sub>H<sub>130</sub>NaO<sub>39</sub>, 1689.8081).

**3.4.6. Pharesinoside F (6).** Colorless gum; [α]<sub>D</sub><sup>25</sup> -30.6 (*c* 1.0, MeOH); IR (KBr) *v*<sub>max</sub> 3438, 2930, 1730, 1632, 1454, 1384, 1076 cm<sup>-1</sup>; <sup>1</sup>H and <sup>13</sup>C NMR data, see Tables 2 and 4; ESIMS *m/z* 1701 [M + Cl]<sup>-</sup> and 1689 [M + NH<sub>4</sub>]<sup>+</sup>; HRESIMS *m/z* 1689.8073 [M + Na]<sup>+</sup> (calcd for C<sub>76</sub>H<sub>130</sub>NaO<sub>39</sub>, 1689. 8081).

**3.4.7. Pharesinoside G (7).** White amorphous powder; [α]<sub>D</sub><sup>25</sup> -45.0 (*c* 1.0, MeOH); IR (KBr) *v*<sub>max</sub> 3416, 2932, 1735, 1637, 1457, 1384, 1071 cm<sup>-1</sup>; <sup>1</sup>H and <sup>13</sup>C NMR data, see Tables 3 and 4; ESIMS *m/z* 1529 [M + Cl]<sup>-</sup> and 1517 [M + Na]<sup>+</sup>; HRESIMS *m/z* 1517.7340 [M + Na]<sup>+</sup> (calcd for C<sub>68</sub>H<sub>118</sub>NaO<sub>35</sub>, 1517.7346).

### 3.5. Alkaline hydrolysis of resin glycoside mixture and preparation of (-)-MTPA ester as authentic samples

Resin glycoside mixture Fr. Cb (2.6 g) was dissolved in 3% K<sub>2</sub>CO<sub>3</sub> (40ml) and heated at 95°C for 2h. After cooling, the reaction mixture was acidified to pH 4.0 with 1 N HCl and extracted successively with CH<sub>2</sub>Cl<sub>2</sub> (40 ml × 3) and Et<sub>2</sub>O (40 ml × 4). Two extracts were washed with water and dried over Na<sub>2</sub>SO<sub>4</sub> to give organic acid fractions. The CH<sub>2</sub>Cl<sub>2</sub> layer organic acid fraction (150 mg) was treated with triethylamine (20 drops) and *p*-bromophenacyl bromide (306 mg) in dry acetone (6 ml) for 1h at room temperature. The mixture was filtered and the filtrate was fractioned between H<sub>2</sub>O (15 ml) and ether (15 ml × 4). The organic phase was further separated by semi-preparative HPLC with MeOH-H<sub>2</sub>O (7:3, *v/v*) to yield *p*-bromophenacyl 2-methylbutyrate (**18**, 62 mg).<sup>21</sup> The same treatment of ether layer organic acid fraction provided *p*-bromophenacyl nilate (10 mg).<sup>21</sup> Two *p*-bromophenacyl esters existed proved the presence of 2-methylbutyric acid and nilic acid units in the original structures.<sup>13</sup> The absolute configuration of 2-methylbutyric acid was identified as *S* by comparison of the <sup>1</sup>H NMR spectrum and specific rotation value ([α]<sub>D</sub><sup>25</sup> +13.6) of *p*-bromophenacyl 2-methylbutyrate with those of the literature data.<sup>21</sup>

*p*-Bromophenacyl 2*S*-methylbutyrate (**18**): Colorless needles; [α]<sub>D</sub><sup>25</sup> +13.6 (*c* 1.5, CHCl<sub>3</sub>); ESIMS *m/z* 300 [M + H]<sup>+</sup>; <sup>1</sup>H NMR (500 MHz, CDCl<sub>3</sub>): δ<sub>H</sub>: 0.98 (3H, t, *J* = 7.4 Hz, H<sub>3-4</sub>), 1.24 (3H, d, *J* = 7.0 Hz, H<sub>3-5</sub>), 1.56, 1.79 (each 1H, m, H-3), 2.56 (1H, m, H-2), 5.28 (2H, s, OCH<sub>2</sub>CO), 7.63 (2H, d, *J* = 8.5 Hz, Ar-H), 7.78 (2H, d, *J* = 8.5 Hz, Ar-H).

*p*-Bromophenacyl nilate: Colorless needles; [α]<sub>D</sub><sup>25</sup> -9.8 (*c* 1.4, CHCl<sub>3</sub>); ESIMS *m/z* 314 [M-H]<sup>-</sup>; <sup>1</sup>H NMR (500 MHz, CDCl<sub>3</sub>): δ<sub>H</sub>: 1.25 (3H, d, *J* = 7.1 Hz, H<sub>3-5</sub>), 1.30 (3H, d, *J* = 6.3 Hz, H<sub>3-4</sub>), 2.62 (1H, dq, *J* = 7.0, 7.0 Hz, H-2), 3.97 (1H, dq, *J* = 7.0, 6.0

Hz, H-3), 5.33, 5.43 (each 1H, d,  $J = 16.5$  Hz, OCH<sub>2</sub>CO), 7.65 (2H, ddd-like,  $J = 8.5, 2.0, 2.0$  Hz, Ar-H), 7.76 (2H, ddd-like,  $J = 8.5, 2.0, 2.0$  Hz, Ar-H).

*p*-Bromophenacyl nilate (2.9 mg) was treated with DMAP (2.8mg), (*R*)-(-)- $\alpha$ -methoxy- $\alpha$ -(trifluoromethyl)-phenylacetyl chloride (7.4  $\mu$ l, 10 mg) in dry pyridine (150  $\mu$ l) and the reaction mixture was left to stand at room temperature until the reaction was complete as evidenced by no more formation of crystalline pyridine hydrochloride.<sup>32</sup> The solvent was removed under a N<sub>2</sub> stream and gave a (-)-MTPA ester after purified by pre-HPLC. The <sup>1</sup>H NMR spectrum with two serial of signals indicated that it was a (-)-MTPA ester mixture of *p*-bromophenacyl-(2*R*, 3*R*)-nilate and *p*-bromophenacyl-(2*S*, 3*S*)-nilate in the ratio of approximately 4:1 based on the signal intensities due to H<sub>3-5</sub> ( $\delta_{\text{H}}$  1.24, 1.31) of the (2*R*, 3*R*)- and (2*S*, 3*S*)-form.<sup>21, 33</sup> HPLC analysis of it on Ultimate SiO<sub>2</sub> column [250  $\times$  4.6 mm, 5  $\mu$ m; solvent, *n*-hexane-isopropanol (4:1, *v/v*)] also have a satisfactory resolution and two peaks ( $t_{\text{R}} = 12.1$  and 10.5 min) with area ratio of 4:1 (S44, Supplementary Data) were consistent with the results of NMR spectrum, thus they were identified respectively as 2*R*, 3*R*- and 2*S*, 3*S*-forms. The (-)-MTPA ester mixture obtained was used as an authentic sample for absolute configuration determination of individual compounds.

The aqueous phase was extracted with *n*-butanol (40ml  $\times$  3) and solvent was removed *in vacuo*. Residue was separated by preparative HPLC with a shim-pack RP-C<sub>18</sub> column (20  $\times$  200 mm) using CH<sub>3</sub>CN:H<sub>2</sub>O with 0.1% formic acid (25:75, *v/v*) to afford pharbitic acid C (**12**) and pharbitic acid D (**13**).

### 3.6. Alkaline hydrolysis and preparation of (-)-MTPA esters of individual compounds for absolute configuration determination

Compounds **1-7** (4 mg each) were dissolved in 3% K<sub>2</sub>CO<sub>3</sub> (0.8-1 ml) and heated at 80°C for 2h. 1N HCl was added to adjust pH to 4 and then extracted with ether (3  $\times$  1ml), respectively. The upper layer was washed with H<sub>2</sub>O and dried over anhydrous Na<sub>2</sub>SO<sub>4</sub>. After removal of reagent, the organic acid residue in dry acetone (0.1-0.2 ml) was neutralized with triethylamine (1-2 drops) and 1.5 mg *p*-bromophenacyl bromide was added to stay at room temperature for 1h. The reaction mixture was concentrated and fractioned with ether to get a residue, which was subjected to HPLC to give *p*-bromophenacyl nilate from **1-7** and *p*-Bromophenacyl 2*S*-methylbutyrate from **4-7**. Each individual solution of *p*-bromophenacyl nilate, DMAP (1.2-1.5mg) and (-)-MTPACI (2  $\mu$ l) in dry pyridine stayed overnight to furnish (-)-MTPA ester, respectively. On the basis of the comparison between each (-)-MTPA ester of *p*-bromophenacyl nilate and the authentic sample mentioned above in the normal-phase HPLC with same analysis conditions [Ultimate SiO<sub>2</sub> column, 250  $\times$  4.6 mm, 5  $\mu$ m; solvent, *n*-hexane-isopropyl alcohol (4:1, *v/v*)], the absolute configurations of nilic acid in the structures were determined as shown (S44, Supplementary Data).

The aqueous phase of **1-7** was separately extracted with *n*-butanol (1 ml  $\times$  3) and the solvent was removed *in vacuo*. Residue was subjected to preparative HPLC with a shim-pack RP-C<sub>18</sub> column (20  $\times$  200 mm) using CH<sub>3</sub>CN-H<sub>2</sub>O with 0.1% formic acid (25:75, *v/v*) to give pharbitic acid B (**14**) from compound **7**, pharbitic acid C (**12**) from compounds **1, 4**, and pharbitic acid D (**13**) from **2-3, 5-6**.

### 3.7. Cytotoxicity assay.

The isolated compounds were evaluated for their cytotoxicities against MDA-MB-231, HCT-116 cell lines by

MTT assay. Cells were plated in 96-well microplates (6,000 cells/well, 200  $\mu$ l) and routinely cultured in a humidified incubator for 24h. The medium was aspirated off and exchanged for medium containing each compound at various concentrations for additional 24h. Then, 20  $\mu$ l MTT (5 mg/ml stock solution) was added to each well and incubated for 4h. After the medium was removed, 150  $\mu$ l DMSO was added to dissolve the formazan crystals by constant shaking for 10 min. The optical density was measured at a test wavelength of 570 nm and a reference wavelength of 630 nm using a Universal Microplate Reader (Spectramax Plus 384, Molecular Devices, Sunnyvale, CA, USA). Cell viability was calculated by the following formula: Cell viability % = (A treatment group/A control group)  $\times$  100%. These differences are expressed in percentage, and cytotoxic activity was indicated as an IC<sub>50</sub> value. The data were presented as the means  $\pm$  SEM for at least three independent experiments.

### 3.8. Antimigration activity

The compounds were further evaluated for their suppression effects on tumor migration with HCT-116 cell line by wound healing and transwell assay.

**Wound healing assay.** Cells (1  $\times$  10<sup>5</sup>/ml) were seeded into a 6-well plate. After incubated for 24h (80-90% confluence), cells were switched to serum-free medium and cultured for another 12h. Then, the cells were gently scratched in the middle of each well with a 10  $\mu$ l plastic pipette tip to create a mechanical wound and incubated with different test substances. Images were taken at 0 and 24h after scraping by a phase-contrast microscope.

**Transwell assay.** The cell migration was determined using a transwell chamber (Corning, USA) with a pore size of 8  $\mu$ m. 5  $\times$  10<sup>4</sup> cells suspended in FBS-free medium were placed in the upper chamber, whereas complete medium was added to the lower chamber. After incubation for 24h at 37 °C, the cells in the upper chamber were carefully removed with a cotton swab, and the cells that had traversed to the reverse face of the membrane were fixed with paraformaldehyde, and stained with crystal violet. Migrated cells were counted by using a phase-contrast microscopy.

### Acknowledgments

This work was supported financially by the National Natural Science Foundation of China (No. 81573570), the project funded by the Priority Academic Program Development of Jiangsu Higher Education Institutions (PAPD), and the Program for Changjiang Scholars and Innovative Research Team in University (IRT\_15R63).

### Supplementary Data

Supplementary data associated with this article can be found in the online version.

### References and notes

- Kinghorn, A. D.; Falk, H.; Kobayashi, J. In *Progress in the Chemistry of Organic Natural Products*; Budzikiewicz, H.; Pereda-Miranda, R.; Rosas-Ramírez, D.; Castañeda-Gómez, J.; Eds.; Springerwien: New York, 2010; Vol. 92, pp 77-153.
- Cao, S. -G.; Guza, R. C.; Wisse, J. H.; Miller, J. S.; Evans, R.; Kingston, D. G. I. *J. Nat. Prod.* **2005**, *68*, 487-492.
- Yin, Y. -Q.; L. Y.; Kong, L. -Y. *J. Agric. Food Chem.* **2008**, *56*, 2363-2368.
- Song, W. -B.; Wang, W. -Q.; Zhang, S. -W.; Xuan, L. -J. *Bioorg. Med. Chem. Lett.* **2015**, *25*, 795-798.
- Bautista, E.; Frago-Serrano, M.; Pereda-Miranda, R. *J. Nat.*

- Prod.* **2015**, 78, 168-172.
6. Figueroa-Gonzalez, G.; Jacobo-Herrera, N.; Zentella-Dehesa, A.; Pereda-Miranda, R. *J. Nat. Prod.* **2012**, 75, 93-97.
7. Ono, M.; Takigawa, A.; Kanemaru, Y.; Kawakami, G.; Kabata, K.; Okawa, M.; Kinjo, J.; Yokomizo, K.; Yoshimitsu, H.; Nohara, T. *Chem. Pharm. Bull.* **2014**, 62, 97-105.
8. Ono, M.; Kawakami, G.; Takigawa, A.; Kabata, K.; Okawa, M.; Kinjo, J.; Yokomizo, K.; Yoshimitsu, H.; Nohara, T. *Chem. Pharm. Bull.* **2014**, 62, 839-844.
9. Bensky, D.; Gamble, A. In *Chinese Herbal Medicine: Materia Medica*; Revised, Ed.; Eastland: Seattle, 1993; p 121.
10. Kawasaki, T.; Okabe, H.; Nakatsuka, I. *Chem. Pharm. Bull.* **1971**, 19, 1144-1149.
11. Okabe, H.; Koshito, N.; Tanaka, K.; Kawasaki, T. *Chem. Pharm. Bull.* **1971**, 19, 2394-2408.
12. ONO, M.; NODA, N.; KAWASAKI, T.; MIYAHARA, K. *Chem. Pharm. Bull.* **1990**, 38, 1892-1897.
13. Ono, M.; Takigawa, A.; Mineno, T.; Yoshimitsu, H.; Nohara, T.; Ikeda, T.; Fukuda-Teramachi, E.; Noda, N.; Miyahara, K. *J. Nat. Prod.* **2010**, 73, 1846-1852.
14. Ono, M.; Akiyama, K.; Yamamoto, K.; Mineno, T.; Okawa, M.; Kinjo, J.; Miyashita, H.; Yoshimitsu, H.; Nohara, T. *Chem. Pharm. Bull.* **2014**, 62, 830-835.
15. Akiyama, K.; Yamamoto, K.; Mineno, T.; Okawa, M.; Kinjo, J.; Yoshimitsu, H.; Nohara, T.; Ono, M. *Chem. Pharm. Bull.* **2014**, 62, 125-133.
16. Fan, B. -Y.; Luo, J. -G.; Gu, Y. -C.; Kong, L. -Y. *Tetrahedron.* **2014**, 70, 2003-2014.
17. Fan, B. -Y.; Gu, Y. -C.; He, Y.; Li, Z. -R.; Luo, J. -G.; Kong, L. -Y. *J. Nat. Prod.* **2014**, 77, 2264-2272.
18. Yu, B. -W.; Luo, J. -G.; Wang, J. -S.; Zhang, D. -M.; Yu, S. -S.; Kong, L. -Y. *J. Nat. Prod.* **2011**, 74, 620-628.
19. Yu, B. -W.; Luo, J. -G.; Wang, J. -S.; Zhang, D. -M.; Yu, S. -S.; Kong, L. -Y. *Phytochemistry.* **2013**, 95, 421-427.
20. Wang, W. -Q.; Song, W. -B.; Lan, X. -J.; Huang, M.; Xuan, L. -J. *J. Nat. Prod.* **2014**, 77, 2234-2240.
21. ONO, M.; TAKAGI-TAKI, Y.; HONDA-YAMADA, F.; NODA, N.; MIYAHARA, K. *Chem. Pharm. Bull.* **2010**, 58, 666-672.
22. Chong, T. T.; Hashim, R.; Bryce, R. A. *J. Phys. Chem. B.* **2006**, 110, 4978-4984.
23. Bogusz, S.; Venable, R. M.; Pastor, R. W. *J. Phys. Chem. B.* **2000**, 104, 5462-5470.
24. Xie, W. -L.; Zhao, L. -L. *Fuel.* **2013**, 103, 1106-1110.
25. Liu, Y.; Zhao, G. -M.; Zhu, W. -C.; Wang, J.; Liu, G.; Zhang, W. -X.; Jia, M. -J. *J. Braz. Chem. Soc.* **2010**, 21, 2254-2261.
26. Werkhoven, P. R.; Elwakiel, M.; Meuleman, T. J.; Quarles van Ufford, H. C.; Kruijtzter, J. A. W.; Liskamp, R. M. J. *Org. Biomol. Chem.* **2016**, 14, 701-710.
27. Fischer, G. M.; Jüngst, C.; Isomäki-Kron Dahl, M.; Gauss, D.; Möller, H. M.; Daltrozzo, E.; Zumbusch, A. *Chem. Commun.* **2010**, 46, 5289-5291.
28. Wang, X. -G.; Lin, K. S. K.; Chan, J. C. C.; Cheng, S. J. *Phys. Chem. B.* **2005**, 109, 1763-1769.
29. Wang, X. -G.; Tseng, Y. -H.; Chan, J. C. C.; Cheng, S. J. *Catal.* **2005**, 233, 266-275.
30. Kubota, Y.; Goto, K.; Miyata, S.; Goto, Y.; Fukushima, Y.; Sugi, Y.; *Chem. Lett.* **2003**, 32, 234-235.
31. Xie, J.; Bogliotti, N. *Chem. Rev.* **2014**, 114, 7678-7739.
32. Dale, J. A.; Mosher, H. S. *J. Am. Chem. Soc.* **1973**, 95, 512-519.
33. Pereda-Miranda, R.; Hernández-Carlos, B. *Tetrahedron.* **2002**, 58, 3145-3154.

Click here to remove instruction text...

## Legends

**Fig. 1** HPLC (RP-C<sub>18</sub>)-ELSD (A) and <sup>1</sup>H NMR (pyridine-*d*<sub>5</sub>) (B) analysis of MeOH-soluble fraction (Fr. C) (i) and subfraction Cb (ii) from the seeds of *P. nil*.

**Fig. 2.** Structures of compounds **1-11**

**Fig. 3.** Structures of compounds **12-19**

**Fig. 4.** Key HMBC correlations of compounds **1** and **7**

**Fig. 5.** Effect of individual compounds on HCT-116 cells migration. HCT-116 cells were treated with or without compounds (12.5 μM) for 24h and then subjected to a wound healing assay.

**Fig. 6.** Wound healing and transwell assay on HCT-116 cells with compound **7** in different concentrations. A. Wound healing assay on HCT-116 cells with compound **7** in different concentrations for 24h and the migration ability of the cells was monitored with an inverted microscope. The wound closure area was calculated by measuring the diminution of the wound bed surface upon time; B. The effect of compound **7** on the migration of HCT-116 was detected by transwell assay. Cells were treated with different concentrations of compound **7** for 24h and detected through crystal violet staining. The cell number from the transwell assay was counted. (\*p < 0.05, compared with the control).